Enzymatic Synthesis of Fluorescent Naphthol-Based Polymers

ARTICLE *in* MACROMOLECULES · SEPTEMBER 1996

Impact Factor: 5.8 · DOI: 10.1021/ma960468f

Enzymatic Synthesis of Fluorescent Naphthol-Based Polymers

R. S. Premachandran,[†] S. Banerjee,[†] X.-K. Wu,[†] V. T. John,*[,†] and G. L. McPherson*[,‡]

Departments of Chemical Engineering and Chemistry, Tulane University, New Orleans, Louisiana 70118

J. Akkara, M. Ayyagari, and D. Kaplan

U.S. Army Soldier Systems Command, Natick, Massachusetts 01760

Received March 28, 1996; Revised Manuscript Received July 8, 1996[⊗]

ABSTRACT: A fluorescent polymer of 2-naphthol is prepared using the oxidative enzyme horseradish peroxidase encapsulated in the microstructured system of AOT/isooctane reversed micelles. The monomer, being amphiphilic, partitions to the oil−water interface with the hydroxyl moieties directed toward the microaqueous core. The enzyme is encapsulated in the water core. The precipitated polymer of naphthol has the morphology of single and interconnected microspheres and is soluble in a range of polar and nonpolar organic solvents. Poly(2-naphthol) shows a fluorescence characteristic of the naphthol chromophore and an additional well-resolved fluorescence attributed to an extended quinonoid structure attached to the polymer backbone. Further evidence of the quinonoid structure is obtained through UV, IR, and NMR spectroscopy. Characteristics of the synthesis and structure of poly(2-naphthol) are compared with those of a less fluorescent polymer, poly(4-ethylphenol).

Introduction

In recent years, fluorescent polymers have attracted considerable attention because of their applications in plastic scintillators,[1] luminescent solar concentrators,[2] high laser resistance materials,[3] laser dyes,[4] and fiber optic sensors.[5] Many fluorescent dyes are known to contain segments obtained from 2-naphthol units, naphthol being a relatively inexpensive raw material.[6] Thus, easily processible fluorescent polymers containing the naphthol chromophore should have potential applications in the above areas. The ability of peroxidase-type enzymes to oxidatively couple phenolic units leads to the possibility of using an enzyme-based approach to synthesize polynaphthols. The enzymatic approach to polymer synthesis is environmentally benign and has the potential of producing polymer in high yields. The feasibility of enzymatically synthesizing polyphenols and polynaphthols in organic solvents was first demonstrated by Dordick and co-workers.[7] Approaches to optimizing reaction conditions for peroxidase-catalyzed polyphenol and poly(aromatic amine) synthesis for applications in electrooptics include conducting the reaction in organic solvents,[8] Langmuir monolayers,[9] and reversed micelles.[10]

Peroxidase-catalyzed polyphenol synthesis follows reaction mechanisms similar to those involved in biological lignin synthesis, where the substrate is more complex, typically a *p*-hydroxy, methoxy-substituted cinnamyl alcohol.[11,12] These polymers have potential in traditional applications of phenol−formaldehyde polymers, viz. in resins and coatings technologies.[13] However, the enzymatically synthesized materials are structurally dissimilar to phenol−formaldehyde polymers due to the absence of intervening methylene groups between the aromatic rings. As a result of direct ring-to-ring connections, the polymers obtained by enzymatic polymerization have an aromatic backbone and are thus conjugated[8] with potential applications in electrooptics.[14−16]

Horseradish peroxidase (HRP) catalysis in the presence of H_2O_2 can be written in the simplified form[17]

$$\text{HRP} + H_2O_2 \rightarrow \text{compound I}$$

$$\text{compound I} + \text{R}-\text{H} \rightarrow \text{R}^* + \text{compound II}$$

$$\text{compound II} + \text{R}-\text{H} \rightarrow \text{R}^* + \text{HRP}$$

Compounds I and II are intermediate states of the enzyme, compound I resulting from a two-electron oxidation of the heme group and compound II resulting from the one-electron reduction of compound I. R−H is the substrate, either the phenolic monomer or the oligomer, and R* is the phenoxy radical species. The overall coupling reaction can be expressed as

$$2\text{R}-\text{H} + H_2O_2 \xrightarrow{\text{HRP}} 2\text{R}-\text{R} + 2H_2O$$

Figure 1 illustrates the phenoxy/naphthoxy radicals and coupling modes that are relevant to the understanding of the structure of poly(2-naphthol) and a simpler alkyl-substituted polyphenol, poly(4-ethylphenol). The enzyme controls only the formation of phenoxy/naphthoxy radicals in the presence of H_2O_2.[18] The polymer chains then grow through radical−radical coupling. Such coupling and radical transfer are influenced by the nature of the phenoxy radical; the catalytic efficiency and growth characteristics additionally depend on the reaction medium.

In this paper, we report the synthesis of poly(2-naphthol) in the microstructured environment of AOT/isooctane reversed micelles, focusing on the luminescence properties of the polymer. Reversed micelles are water-in-oil microemulsions where the catalytic enzyme is encapsulated in the microaqueous pools and retains its catalytic activity. An interesting aspect of polyphenol synthesis in reversed micelles is the intrinsic interfacial nature of the reaction. The phenolic substrate, being amphiphilic, partitions to the oil−water

* To whom correspondence may be addressed. V.T.J.: Phone 504-865-5883, Fax 504-865-6744, e-mail vj@che.che.tulane.edu.
[†] Department of Chemical Engineering, Tulane University.
[‡] Department of Chemistry, Tulane University.
[⊗] Abstract published in *Advance ACS Abstracts,* September 1, 1996.

S0024-9297(96)00468-8 CCC: $12.00

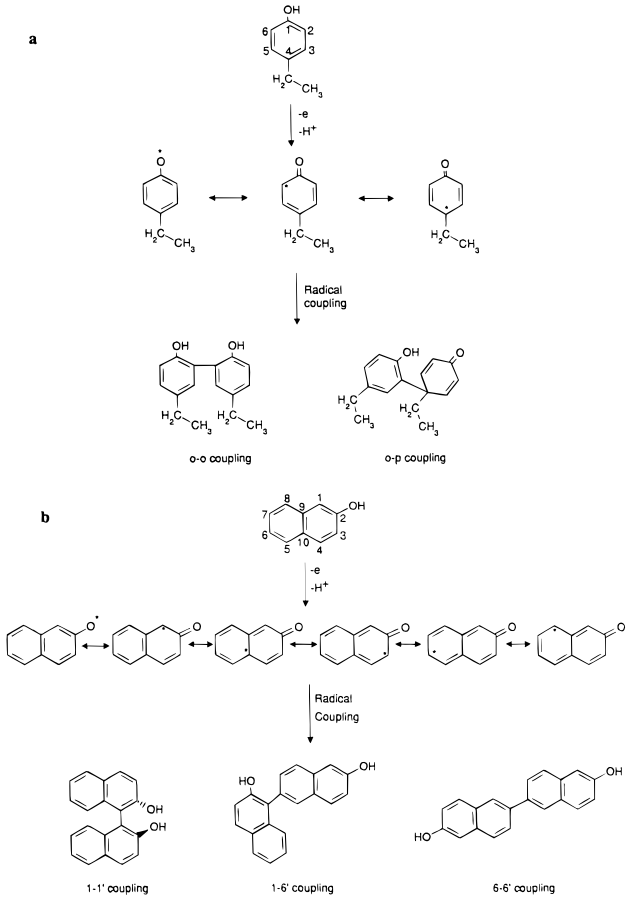

Figure 1. Various radical resonance structures resulting from one-electron oxidation of (a) 4−ethylphenol and (b) 2-naphthol in the presence of HRP and H_2O_2. Since so many positions are activated (especially with 2-naphthol), only some illustrative coupling products are shown.

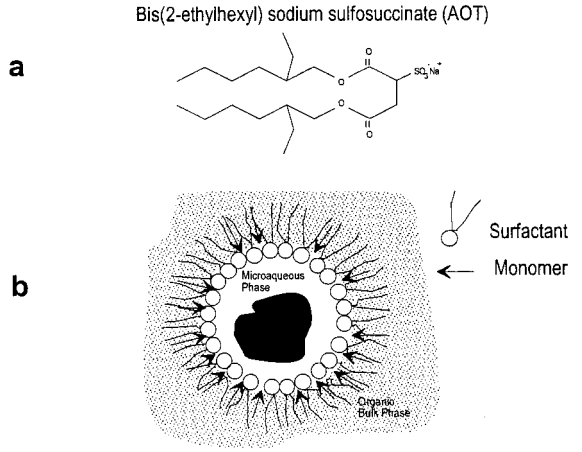

Figure 2. (a) Structure of sodium bis(2-ethylhexyl) sulfosuccinate and (b) schematic of the reversed micelle environment with encapsulated enzyme, illustrating monomer partitioning to the micellar interface.

interface, and it is likely that initial chain growth occurs at the micelle interface. Figure 2 illustrates the situation. The structure of the twin-tailed anionic surfactant sodium bis(2-ethylhexyl) sulfosuccinate, commonly known as AOT, is shown in Figure 2a. Figure 2b illustrates the micelle environment with the encapsulated enzyme. The phenol is represented by the arrow, with the polar hydroxyl groups pointing to the water core of the micelle.

Our earlier work has shown the feasibility of the polymerization of alkyl-substituted phenols (4-ethylphenol) in reversed micelles.[19] This work is therefore an extension, where a fluorescent monomer is deliberately chosen to synthesize a fluorescent polymer. Chemical and morphological comparisons between poly(2-naphthol) and poly(4-ethylphenol) are made in this paper. GPC, FTIR, SEM, NMR, UV, and fluorescence spectroscopy were used to characterize these polymers. These comparisons help in understanding the origins of the luminescence characteristics observed with poly(2-naphthol).

Materials and Methods

Horseradish peroxidase Type II (HRP) and hydrogen peroxide were obtained from Sigma Chemical Co. (St. Louis, MO). The monomers, 4-ethylphenol and 2-naphthol, 1,1′-bi-2-naphthol (a racemic mixture), and the anionic surfactant sodium bis(2-ethylhexyl) sulfosuccinate (AOT) were purchased from Aldrich Chemical Co. (Milwaukee, WI). The solvent isooctane was ACS reagent grade and was also obtained from Aldrich. 2-Naphthol was purified by repeated crystallization in benzene before its use in synthesis.

Polymer Synthesis. The monomer (2-naphthol or 4-ethylphenol; 0.15 M) was dissolved in a reversed micellar system containing 0.5 M AOT in isooctane. To the above solution was added, the required volume of enzyme-containing HEPES buffer (0.01 M, pH 7.5) to bring the micellar water content to a w_0 value of 15 (w_0 is the water to surfactant molar ratio). The enzyme level in the buffer was adjusted so that the final enzyme concentration in the overall micellar solution was 0.5 mg/mL. Reactions were conducted at ambient temperature.

Polymerization was initiated with addition (in aliquots) of the stoichiometric amount of hydrogen peroxide required for complete monomer conversion (0.15 M). The solution turns greenish yellow with instantaneous precipitation of the polymer. Although most of the monomer conversion is completed within 10−15 min of reaction initiation, the solution was kept stirred for 24 h. The polymer was recovered, washed thoroughly with isooctane to remove adsorbed surfactant, air-dried, and stored.

Polymer Characterization. The polymer morphology was characterized by scanning electron microscopy (SEM). For SEM analysis, a drop of the sample dispersed in isooctane was placed on an aluminum stub, dried, and coated first with 20 nm thickness carbon black and then with gold. The micrograph was taken at an acceleration voltage of 15−30 kV in a JEOL JSM-820 scanning electron microscope.

Molecular weight distributions of the polymers were measured using gel permeation chromatography (GPC). The setup consisted of a 25 cm Jordi Gel DVB mixed-bed column, a Perkin-Elmer biocompatible binary pump (Model 250), and a Perkin-Elmer diode array detector (Model 235) interfaced with a personal computer. The eluent was THF, and the column was operated under the eluent head pressure adjusted to maintain the flow rate of 0.75 mL/min. The dry polymer was dissolved in THF at a concentration of 0.1% (w/v), and 20 μL of this solution was used for the measurements. Polystyrene samples in the molecular weight range 600−200 000 were used as calibration standards.

An ATI-Mattson Galaxy 6021 FTIR spectrometer was used for FTIR measurements. A liquid sample cell (SpectraTech) with CaF_2 windows and path length 0.3 mm was used to measure liquid samples. KBr pellets made from a 1% (by weight) polymer/KBr mixture were used for recording the spectra of the polymers. The UV−Vis spectra of the polymers and copolymers were recorded using a Shimadzu UV-160 spectrometer. The fluorescence spectra of the monomer and polymer were recorded using a Perkin-Elmer luminescence spectrophotometer (Model LB-50) equipped with a Xe lamp as the excitation source. The emission slit was kept at 2.5 nm in all measurements. Typical scan rates were 200 nm/min, and the typical concentration used was 0.1g/L.

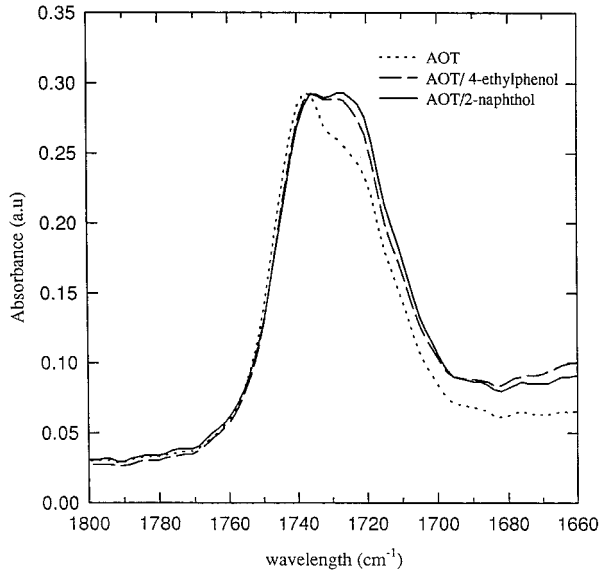

Figure 3. Monomer penetration to the micellar interface is shown by the perturbation in surfactant carbonyl vibrations as a result of surfactant−monomer hydrogen bonding. AOT/isooctane reversed micelles, w_0 ([water]/[AOT]) = 2, [AOT] = 0.05 M, [4-ethylphenol] = 0.03 M, [2-naphthol] = 0.03 M.

High-resolution NMR spectra were recorded on a General Electric Model GE 500 Omega FT-NMR spectrometer operating at 500.05 MHz for protons and 125.75 MHz for ^{13}C. Data acquisition was continued until a reasonable noise/signal ratio was achieved. All spectra were recorded in deuterated DMSO.

Results and Discussion

General Reaction Characteristics. In AOT-based reversed micelles, phenolic monomers partition to the water−oil interface. The subsequent reaction is an example of interfacial polymerization. Figure 3 provides evidence for penetration of the monomer to the micelle interface through the perturbations of the surfactant carbonyl vibrations as a function of monomer concentrations. The low-frequency shift in AOT carbonyl vibrations is a result of hydrogen bonding between these groups (the acceptor) and the monomer hydroxyl groups (the donor). The ability of the monomer to influence surfactant head group vibrational frequencies is assumed to be evidence of monomer penetration to the interfacial region. It is interesting to note that both 2-naphthol and 4-ethylphenol have relatively equivalent effects on the carbonyl frequencies. A qualitative aspect of the interaction of 2-naphthol with AOT is the fact that the surfactant significantly increases the solubility of the monomer in isooctane. With 0.5 M AOT, an eightfold increase in monomer solubility is observed.

As a general characteristic of polymerization in reversed micelles, 2-naphthol polymerization proceeds as efficiently as the polymerization of 4-ethylphenol. In both cases, polymer yields above 95% are obtained. The molecular weight distributions of 2-naphthol and 4-ethylphenol polymers are shown in Figure 4. The peak molecular weight of poly(4-ethylphenol) is 1400 and that of poly(2-naphthol) is approximately 800, indicating the presence primarily of oligomers. Here we must make a correction from our previous work where much higher molecular weights have been measured for poly(4-ethylphenol).[19] The earlier work was in error, perhaps due to rapid elution of polymer aggregates that may have formed as a result of intermolecular hydrogen bonding. Recent work by Ayyagari and co-workers[20] has shown that breaking up polymer aggregates with LiBr

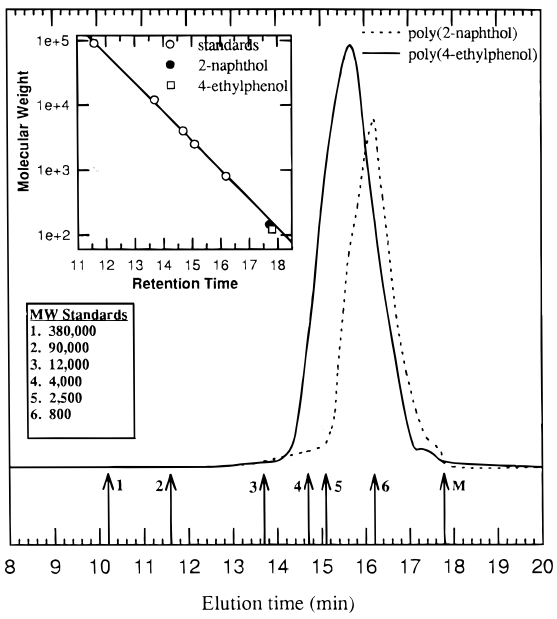

Figure 4. Gel permeation chromatograms for poly(2-naphthol) and poly(4-ethylphenol). The inset shows the retention time versus molecular weight calibration plot made with the polystyrene standards.

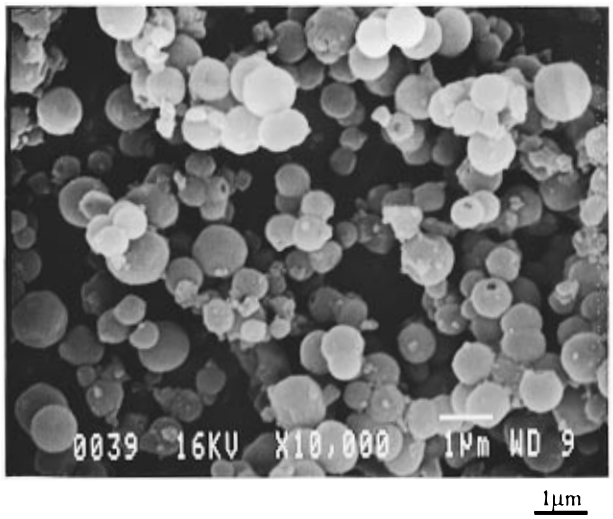

Figure 5. Scanning electron micrograph of poly(2-naphthol) synthesized in reversed micelles.

in a DMF/methanol eluent results in accurate molecular weights. In the present work, we have used THF as the eluent (since the detector flow cell is incompatible with DMF), and the results are in essential agreement with those of Ayyagari and co-workers.[20] Molecular weight determinations have been carried out at the laboratories of both sets of researchers for verification.

Polymer Morphology. Synthesis in the reversed micellar environment leads to polymers that rapidly phase-separate and precipitate out of solution. Interestingly, the recovered poly(2-naphthol) has a microspherical morphology (Figure 5) where polymer particles exist both as distinct and as interconnected microspheres. The morphological characteristics are similar to those of poly(4-ethylphenol)[19] and are reproducibly obtained when a 3/1 (or greater) molar ratio of surfactant to monomer is used in the synthesis. Studies to delineate the morphology development and internal structure of the microspheres are in progress.

Absorption and Fluorescence Properties. Figure 6 illustrates the UV−vis absorption characteristics of

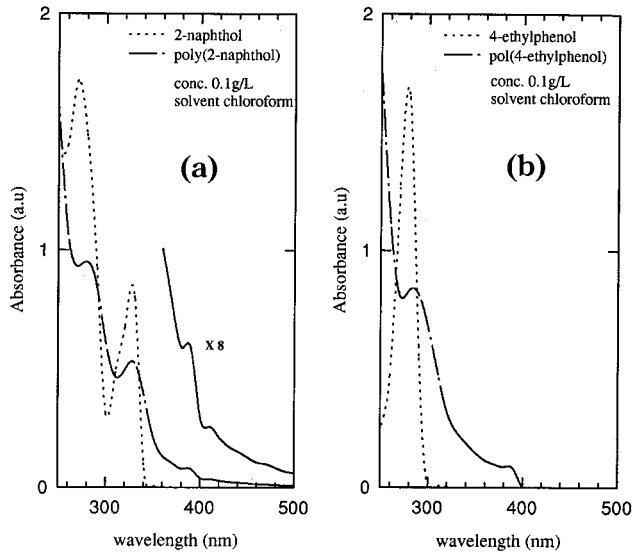

Figure 6. UV−Visible absorption spectra of (a) 2-naphthol and poly(2-naphthol) and (b) 4−ethylphenol and poly(4-ethylphenol). The inset of (a) shows an 8× magnified view of the tail region in the absorption spectra of poly(2-naphthol). The presence of the n−π* absorption maximum is seen in the expansion.

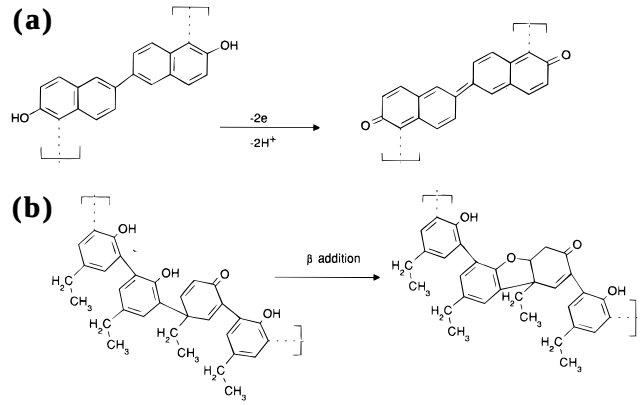

Figure 7. Postulated quinonoid and ketonic structures for (a) poly(2-naphthol) and (b) poly(4−ethylphenol). Such segments either may be present as end groups or may be present within the chain.

both monomers and their corresponding polymers. The absorption spectrum of 2-naphthol indicates two strong absorption peaks centered at 270 and 330 nm, while 4-ethylphenol exhibits a single peak at 280 nm. These bands are assigned to the $\pi-\pi$* transitions in phenols.[21] The absorption spectrum of poly(2-naphthol) shows the peaks at 270 and 330 nm slightly red-shifted and a tail region, all of which can be attributed to conjugation in the polymer. The same is true with poly(2-ethylphenol), where there is an extended tail absorption. There are, however, additional features in the absorption spectrum of the two polymers. With both polymers, a clear peak is seen at 390 nm; with poly(2-naphthol), a very weak peak is additionally seen around 410 nm (shown more clearly in the 8× expansion). These peaks cannot be ascribed to the aromatic moieties and indicate heterogeneity in polymer structure and the possible presence of additional absorbing groups. Figure 7 illustrates these mechanistic possibilities. For example, poly(2-naphthol) may be formed due to 1−1′, 1−6′, and 6−6′ coupling of the monomers (Figure 1). However, if 6−6′ coupling occurs, this moiety on the chain can undergo further oxidation to the quinonoid form shown in Figure 7a. Similarly, poly(4-ethylphenol) may be formed primarily due to *o*−*o* coupling (Figure 1b). However, *o*−*p* coupling and subsequent rearrangement as shown in Figure 7b may lead to ketonic structures incorporated into the chain. The ketonic moiety arising from *o*−*p* coupling in the polymerization of 4-ethylphenol is Pummerer's ketone, and its formation in HRP-catalyzed oxidation of cresols was been reported as early as 1942.[22]

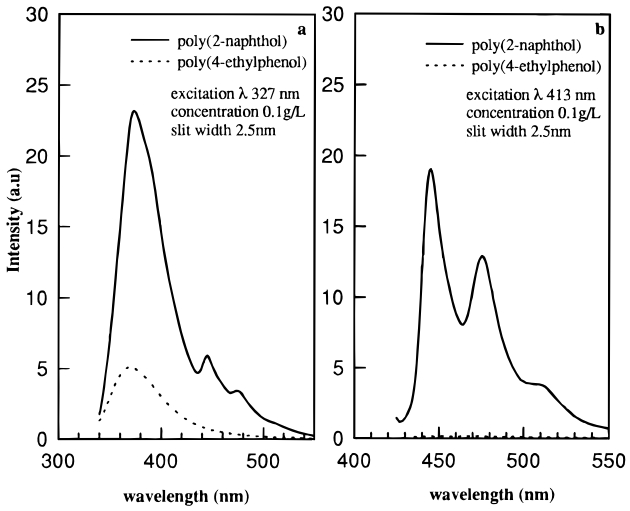

Figure 8. Fluorescence spectra in chloroform of (a) poly(2-naphthol) and poly(4-ethylphenol) excited at 327 nm and (b) the same polymers excited at 413 nm. Poly(4-ethylphenol) shows a weak fluorescence when excited at 327 nm and no emission when excited at 413 nm.

Additional evidence that the peaks at 390 and 415 nm in Figure 6a correspond to transitions in quinonoid segments in poly(2-naphthol) is based on the assignment of absorption maxima for various quinones reported in the literature.[23−25] In polycyclic quinones, the electronic transitions must be treated as local transitions in fragments. Para-substituted quinones have three distinct absorptions, one at 240−285 nm, the second at 285−385 nm, and a third at 385−460 nm.[26] The first two bands are attributed to the $\pi-\pi$* transitions of the aromatic fragments, while the third band is attributed to the n−π* transitions in the carbonyl group. The third band is much less prominent due to the forbidden nature of the n−π* transition. In Figure 6a, therefore, the small humps at 390 and 410 nm may be attributed to such n−π* transitions in quinonoid carbonyl groups superimposed on the tail of the $\pi-\pi$* absorbances. In summary, the peaks at 270 and 340 nm in poly(2-naphthol) are assigned to the aromatic $\pi-\pi$* transitions of both naphtholic and quinonoid moieties, while the 390 and 415 nm peaks are assigned to n−π* transitions in the quinonoid carbonyl groups superimposed on the $\pi-\pi$* tail absorbances. We use a similar argument to propose that the small peak at 390 nm in Figure 6b for poly(4-ethylphenol) arises from the n−π* transition in the carbonyl group of Pummerer's ketone moieties.

The fluorescence spectra in solution (chloroform solvent) provide the essential evidence on which the structural arguments are based. Poly(2-naphthol) on excitation at 327 nm (the excitation maximum for the monomer) exhibits an emission spectrum with an intense peak at 375 nm and two other peaks of much lower intensity centered around 455 and 481 nm (Figure 8a). The monomer, 2-naphthol, and the dimer, bi-2-naphthol, show emission maxima at 355 and 358 nm, respectively, characteristic of the naphthol moiety.[27] Thus, the band at 375 nm in poly(2-naphthol) can be assigned to naphthol residues within the polymer, with

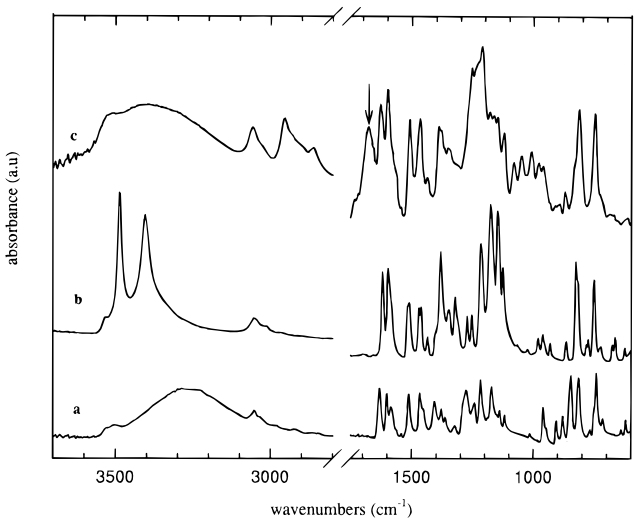

Figure 9. FTIR spectra of (a) 2-naphthol, (b) 1,1′-bi-2-naphthol, and (c) poly(2-naphthol). The spectrum of 1,1′-bi-2-naphthol is included for comparison. The position of the C═O stretch possibly arising from quinonoid segments is marked by an arrow. The region 3200−1700 cm^{-1} is not shown since there are no characteristic bands in this region.

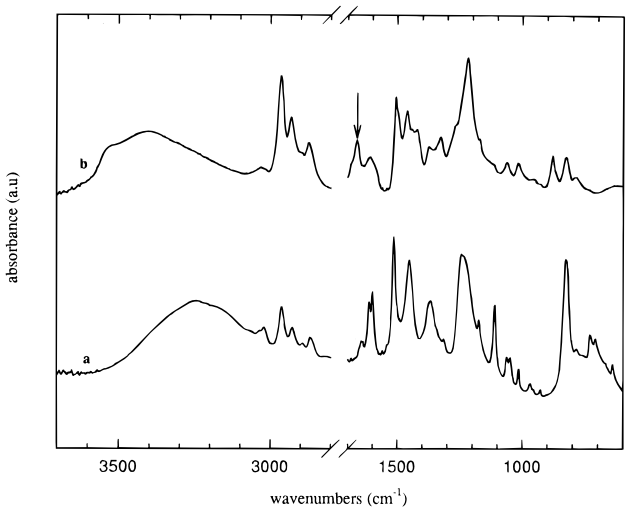

Figure 10. FTIR spectra of (a) 4-ethylphenol and (b) poly(4-ethylphenol). The position of the C═O stretch, possibly arising from Pummerer's ketone segments, is marked by an arrow. The region 3200−1700 cm^{-1} is not shown since no characteristic bands are present in this region.

the 20 nm red shift from the monomer to the polymer attributed to the increase in conjugation.

The emission intensities at 455 and 481 nm become significantly stronger when poly(2-naphthol) is excited at 413 nm. Excitation at 413 nm reveals a well-structured and highly reproducible emission with intense peaks at 455 and 481 nm (Figure 8b). These bands cannot be assigned to naphthol units, and the bands represent emitting states distinct from the naphthol $\pi-\pi^*$ singlet state. It cannot be an excimer or exiplex as the emission from such bimolecular aggregates consists of broad structureless bands to the low-energy side of normal fluorescence. Also, the emission profile of such a complex would not be dependent on the excitation wavelength within the $\pi-\pi^*$ band of the polymer. The fact that the long-wavelength band can be observed by direct excitation indicates that the chromophore which gives rise to the emission exists in the ground state. One possibility is that the fluorescence results from a more conjugated chromophore bound within the polymer. Again, returning to Figure 7a, the rigid, planar, conjugated structures of the quinonoid segments in the chain indicate the possibility that these are the fluorophores giving rise to the emission with features at 455 and 481 nm. Since fluorescence is sensitive even to trace concentrations of highly fluorescent groups in a polymer backbone when appropriately excited, it is possible that even small amounts of these fluorophores may be responsible for the structured emission at 455 and 481 nm.

Poly(4-ethylphenol) shows a weak fluorescence band around 365 nm, again characteristic of the phenolic residues (Figure 8a). However, there is no additional emission. This observation can be mechanistically rationalized. Unlike the quinonoid structure formed in the case of poly(2-naphthol), the Pummerer's ketone type groups shown in Figure 7b are nonplanar and thus should show very weak fluorescence, characteristic only of the benzenoid fragment.[27]

Characterization by FTIR Spectroscopy. Figure 9 illustrates the FTIR spectra of (a) 2-naphthol, (b) bi-2-naphthol, and (c) poly(2-naphthol), and Figure 10 the FTIR spectra of (a) 4-ethylphenol and (b) poly(4-ethylphenol). Peak identifications were made using data reported in the literature[28] and are listed in Table 1 for additional clarity in reporting the spectra. The following are aspects of the spectra relevant to polymer structure. First, the retention of a strong OH stretch region in both poly(2-naphthol) and poly(2-ethylphenol) indicates that the polymer has significant phenol/naphthol character. In both polymers, the OH stretch region is shifted to higher frequencies relative to the monomer. This is probably due to weaker hydrogen-bonding interactions between the hydroxyl groups in the polymer relative to self-associations arising in the monomer. A second observation is related to the bands in the 900−650 cm^{-1} regions, arising from CH out-of-plane bending frequencies. These bands are very characteristic of substitution patterns in an aromatic ring.[28] In the case of 4-ethylphenol (Figure 10a) the band corresponding to the CH out-of-plane bend at 825 cm^{-1} shows the presence of two adjacent hydrogen atoms in the benzene ring. On polymerization (Figure 10b), the band intensity at 825 cm^{-1} decreases considerably and another new peak appears at 879 cm^{-1}, which is characteristic of the out-of-plane bend corresponding to a lone hydrogen atom. Thus the new band at 879 cm^{-1} may be assigned to CH out-of-plane vibrations for a 1,2,4,6-tetrasubstituted aromatic ring.[28] This is indirect evidence that the polymerization of the phenol units may proceed primarily via ortho−ortho coupling. The dominance of ortho−ortho coupling has also been reported in earlier studies on polyphenol synthesis in monophasic organic solvents.[8,20,29] The IR spectrum of 2-naphthol (Figure 9a) in this region shows bands at 844, 814, and 742 cm^{-1}, which are characteristic of out-of-plane CH bends of a naphthalene ring with one, two, and four adjacent hydrogens, respectively. The band at 844 cm^{-1}, corresponding to the CH out-of-plane bend for a lone hydrogen, disappears on polymerization (Figure 9c and Table 1), indicating that the 1 position is involved in polymerization. The other bands are retained at 814 and 748 cm^{-1}, respectively. On comparison with the equivalent bands for bi-2-naphthol (at 825 and 752 cm^{-1}), the small shifts can be explained through an increased restriction in motion. It is difficult to claim conclusively that there are other linkages in addition to C−C linkages. C−O linkages leading to naphthoxy ether type units are a possibility. However,

Table 1. Vibrational Spectra Assignments of Various Monomers and Polymers

description	*p*-ethylphenol	poly(ethylphenol)	2-naphthol	polynaphthol	bi-2-naphthol
OH stretch	3254 (s)	3408 (s)	3286 (s)	3406 (s)	3487 (s)
					3404 (s)
CH stretch (aromatic)	3022 (w)	3032 (w)	3053 (w)	3057 (w)	3053 (w)
CH_3 and CH_2	2962 (s)	2964 (s)			
stretch (aliphatic)	2928 (s)	2931 (s)			
	2868 (m)	2872 (m)			
C═O stretch		1662 (m)		1678 (m)	
C═C stretch	1612 (m)	1610 (m)	1631 (m)	1628 (m)	1618 (m)
aromatic	1599 (m)	1504 (s)	1601 (m)	1599 (m)	1597 (m)
	1514 (s)	1460 (s)	1512 (s)	1508 (s)	1510 (s)
	1450 (s)		1467 (s)	1465 (s)	1462 (s)
in-plane OH bend	1365 (s)	1373 (m)	1379 (s)	1388 (s)	1381 (s)
C−OH stretch	1242 (s)	1217 (s)	1217 (s)	1213 (s)	1217 (s)
C═O asymmetric		1060 (w)		1080 (w)	
vibration				1049 (w)	
out-of-plane CH bend	825 (s)	825 (m)	844 (s)	812 (s)	825 (m)
		879 (m)	814 (s)	748 (s)	752 (m)
			742 (s)		

the formation of such ether linkages should produce a characteristic band for aromatic ethers (Ar−O−Ar) around 1270−1280 cm^{-1}, which is not observed. The polymer still retains vibrational bands corresponding to free naphthol hydroxyl groups (phenolic CO stretch at ∼1210 cm^{-1} and the OH stretch between 3100 and 3500 cm^{-1}), indicating its essentially naphthol nature.

Finally, tentative evidence for quinonoid groups and ketonic groups is seen through new C═O vibrations that arise on polymerization. For poly(2-naphthol) these vibrations are observed at 1676 cm^{-1} (the arrow in Figure 9c), and for poly(4-ethylphenol) the vibrations are at 1662 cm^{-1}(the arrow in Figure 10b). We attribute the C═O vibrations in poly(2-naphthol) to the quinonoid segments of the polymer that can arise from the oxidation of 6−6′ coupled units (Figure 7a) and corroborate IR data reported for the electrochemical oxidation of 2-naphthol which also postulate the possible formation of quinonoid moieties.[30] In the case of poly(4-ethylphenol), the C═O vibrations are attributed to Pummerer's ketone segments (Figure 7b). There is also a decrease in band intensity for the in-plane OH bend at 1365 cm^{-1}, implying that some OH groups may be lost during polymerization. The observation may be supporting evidence for the formation of Pummerer's ketone.[31] However, the retention of the strong hydroxyl stretch (3100−3600 cm^{-1}) indicates the essentially phenolic nature of the polymer.

Characterization by NMR Spectroscopy. The ^1H NMR spectra of 2-naphthol and the individual proton assignments are shown in Figure 11a. As shown in Figure 1b, there are several possibilities for naphthoxy radical coupling. The possible existence of a multitude of coupling modes within one single polymer chain makes it difficult to choose a model repeat unit for study. However, since the 1−1′ coupling is generally favored, we have included the ^1H NMR of 1,1′-bi-2-naphthol to compare spectral characteristics. The spectra and assignment of various protons in bi-2-naphthol are depicted in Figure 11b. The ^1H NMR of poly(2-naphthol) in Figure 11c consists of a series of sharp resonances superimposed on two rather broad absorptions centered at 7.3 and 7.85 ppm (Figure 11c). The vast majority of the total integrated intensity is associated with the broad absorptions. A number of the sharp features appear to correspond to resonances from 2-naphthol and 1,1′-bi-2-naphthol, both of which may have coprecipitated with the polymeric material. The broad features in the spectrum appear to be a manifestation of a number of closely spaced and overlapping individual proton resonances. This is to be expected since there are likely to be many similar but distinct proton resonances in the polymeric material, which appears to contain a range of oligomers. High-temperature spectra (100 °C) do not show improved resolution, a further indication that the broadness is not a consequence of slow rotation of the polymer but an intrinsic consequence of multiple resonances. The peaks observed further upfield (<6.8 ppm) are not due to aromatic hydrogens and may be tentatively assigned to the various alkenic protons in a quinonoid segment.

The ^{13}C spectra of 2-naphthol, 1,1′ bi-2-naphthol, and poly(2-naphthol) are shown in Figure 12a−c, respectively. The ^{13}C spectra are somewhat better resolved than the ^1H spectra and are perhaps a bit more informative. In poly(2-naphthol), resonances observed from 109 to 130 ppm are attributed to the aromatic carbons, in analogy to the monomer and bi-2-naphthol. Those from 146 to 160 ppm are chemical shifts arising from the carbon atoms to which an OH group is attached and may also reflect some of the carbon atoms in quinonoid segments. These assignments are based on values reported for quinonoid-type species in the literature[32−34] and from ^{13}C simulation software (Softshell International, ^{13}C NMR module). Figure 13 illustrates the simulation results for the proposed quinonoid segment, with the peaks downfield of 140 ppm shown in boldface. A precise assignment of the peaks is not possible because the calculated values of chemical shifts are only accurate to ±5 ppm. However, the simulation does provide useful insight about the assignment of chemical shifts. Well-defined resonances from the carbonyl carbons in the quinonoid structure could not be detected in the 180−190 ppm region, except for a possible, very weak feature at 190 ppm which was difficult to distinguish from the noise level. The inset in Figure 11c shows an expansion of this region, with the peaks around 170 ppm arising from the AOT carbonyl carbons (when a 3:1 AOT/naphthol ratio was used, there was always a little contamination of the polymer with AOT, even after repeated washing). The lack of a strong resonance is evidence that the quinonoid groups are in relatively low concentrations. It should also be noted that ^{13}C resonances for ketonic carbons are often weak; the lack of attached hydrogen leads to inefficient spin−spin relaxation and long relaxation times. The difficulty in getting a good signal for ketonic carbons in polymers has recently been noted by Curtis and McClain in studies on the synthesis of poly(thienylene ketone)s.[35] In comparing the resonances of

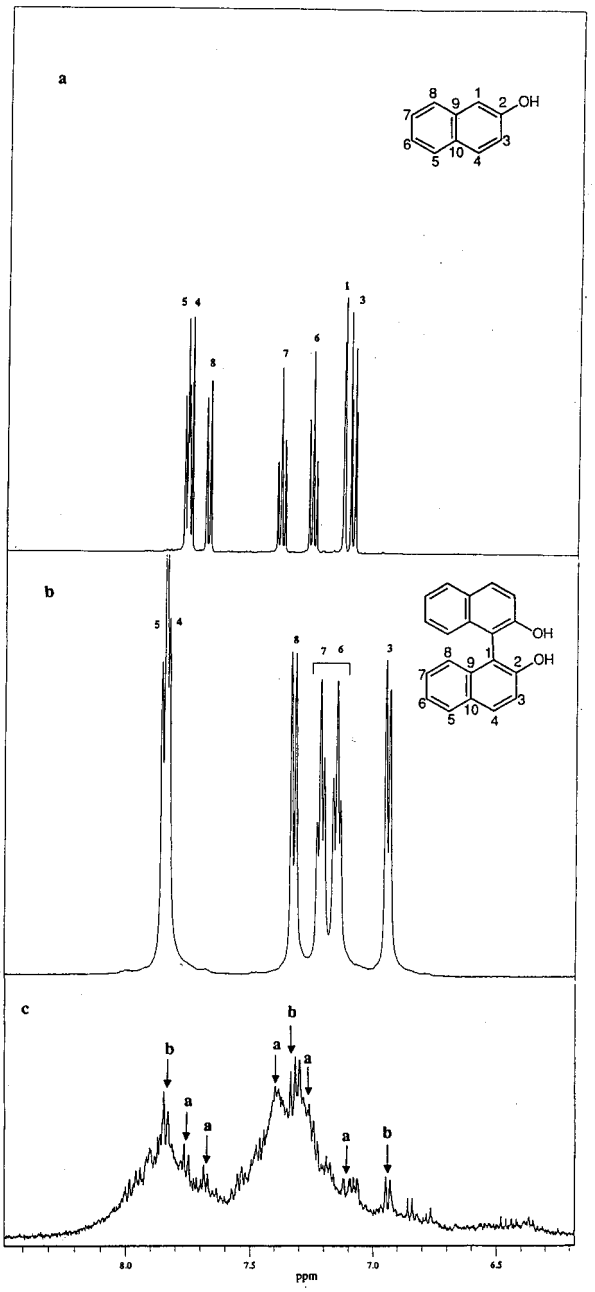

Figure 11. ^{1}H NMR spectra of (a) 2-naphthol, (b) 1,1′-bi-2-naphthol, and (c) poly(2-naphthol). The proton assignments for 1,1′-bi-2-naphthol are deduced based on splitting patterns and comparison with the spectrum for 2-naphthol. In spectrum c, the notations "a" and "b" refer to resonances from 2-naphthol and 1,1′-bi-2-naphthol, respectively. These species represent less than 5% of the integrated area.

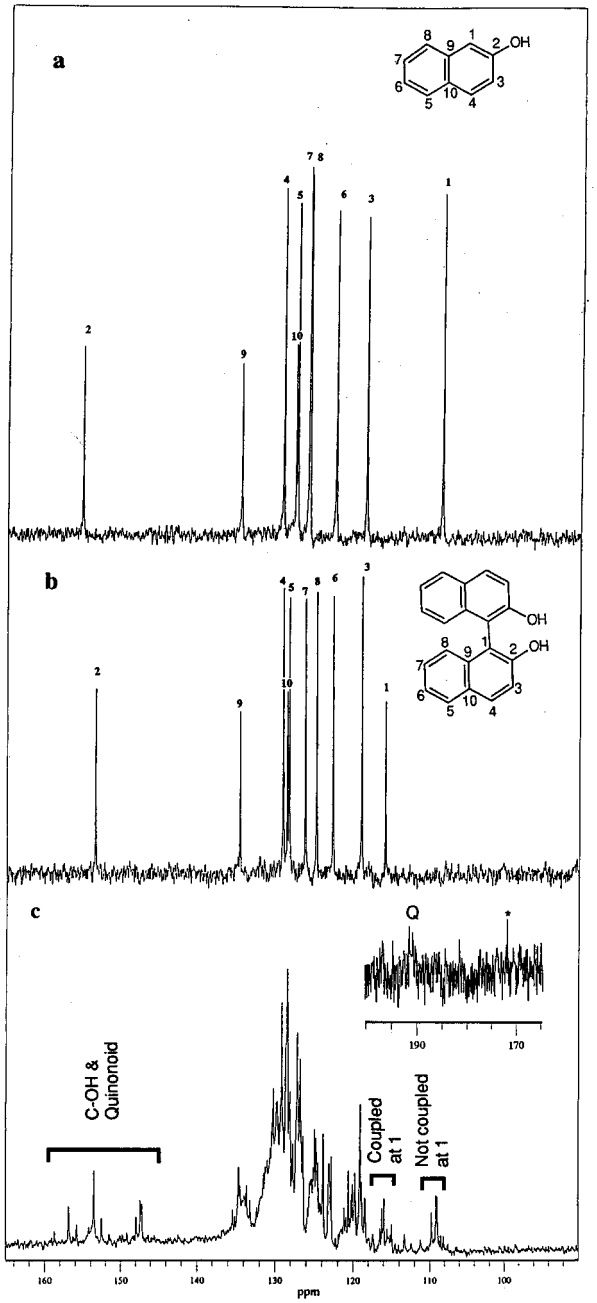

Figure 12. ^{13}C NMR spectra of (a) 2-naphthol, (b) bi-2-naphthol, and (c) poly(2-naphthol). The inset in (c) is the expanded region where the resonance from the carbonyl carbon in the quinonoid segment should appear. A weak feature is noted around 190 ppm (Q). The asterisk corresponds to residual AOT carbonyl carbon resonance.

2-naphthol to those of 1,1′-bi-2-naphthol, it is apparent that 1−1′ coupling shifts the C-1 resonance downfield and reduces the intensity by roughly 40%. There is a less dramatic but noticeable upfield shift in the resonance of the OH carbon (C-2). The spectrum of the polymer shows the presence of a multiplicity of C-1 carbons in naphthol groups coupled at the 1-position and naphthol groups not coupled at the 1-position. The resonances from the OH carbons show a similar multiplicity. As with the proton spectra, there are features attributable to 2-naphthol and 1,1′-bi-2-naphthol. Both ^{13}C and ^{1}H NMR spectra are consistent with a polymeric material composed of relatively small, naphthol oligomers (trimers and tetramers) coupled at different positions. While 1−1′ coupling may be somewhat favored, other modes of coupling must also occur. In summary, the NMR data do not conclusively prove the presence of quinonoid segments but do show the existence of C−C coupling besides the 1−1′ mode.

The ^{1}H NMR spectra of 4-ethylphenol and its polymer are shown in Figure 14. The NMR spectrum of poly(4-ethylphenol) shows two mutually overlapping broad bands centered around 7.0 and 6.8 ppm arising from aromatic protons. The broad peaks around 1.0 and 2.5 ppm can be assigned to methyl and methylene protons. The small but sharp peaks at 5.9, 5.0, and ∼3.0 ppm are perhaps protons in the Pummerer's ketone structure.[36]

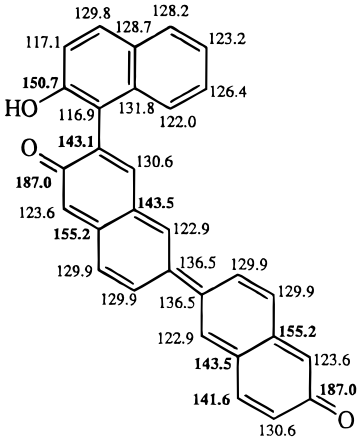

Figure 13. Calculated ^{13}C NMR chemical shifts (ppm) for a model quinonoid segment. The carbons giving rise to resonances above 140 ppm (i.e. downfield of 140 ppm) are shown in boldface. The calculations are accurate only within an error margin of ±5 ppm.

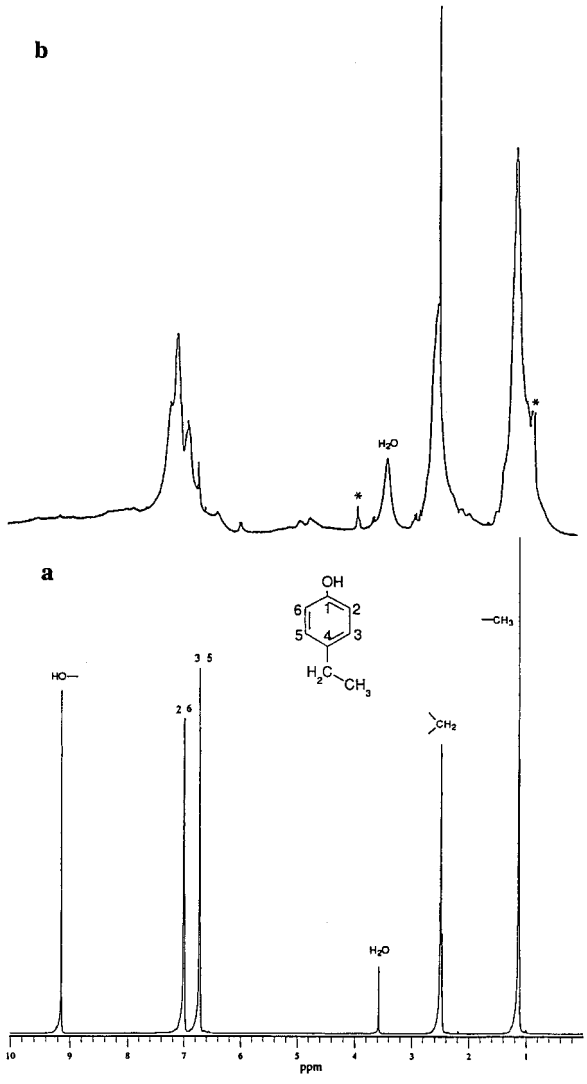

Figure 14. ^1H NMR spectra of (a) 4-ethylphenol, and (b) poly(4-ethylphenol). The assignments for the various resonances in the monomer are made as shown. The features marked by the asterisk in the polymer spectrum arise from residual AOT trapped inside the polymer matrix. The resonances around ~6.0 ppm and from 4.5 to 5.0 ppm possibly arise from the protons present in the furanoid ring of Pummerer's ketone.

Conclusion

The species obtained from HRP-catalyzed oxidations of 2-naphthol and 4-ethylphenol are principally oligomers with coupling at various positions of the aromatic ring; to term them polymers is simply a matter of convenience. Poly(2-naphthol) prepared enzymatically in reversed micelles exhibits fluorescence characteristic of naphthol moieties and a second, reproducible and structured emission originating from a highly conjugated chromophore. Careful structural investigation of this polymer using IR and NMR spectroscopy indicates the possible presence of an extended quinonoid structure, perhaps as a minor component within the polymer backbone. By inference, the second emission, observed in the wavelength region 450−480 nm, is attributed to these quinonoid segments. The polymer is not soluble in water or in alkanes but is soluble in many other solvents (acetone, THF, ACN, DMSO, benzene, etc.), both polar and nonpolar. These characteristics indicate a noncross-linked and easily processible material. Additionally, the polymer is synthesized in microspherical morphology, indicating an ease in dispersing the material for coatings applications.

Poly(4-ethylphenol) prepared by the same route does not fluoresce at high wavelength. Spectroscopic characterization indicates the presence of small amounts of Pummerer's ketone type moieties possibly attached to the phenol backbone. The Pummerers ketone moieties are nonconjugated and out-of-plane from connecting aromatic rings. Poly(4-ethylphenol) is therefore not a strongly fluorescing polymer. The enzymatic route to synthesizing fluorescent polymers in micellar systems therefore appears very feasible. In addition to the expected emission, additional features can be generated through the formation of quinonoid units. The possibility of tailoring such emission using various monomers (e.g. hydroxypyrene) or copolymer compositions is an area of continuing study.

Acknowledgment. Financial support from the National Science Foundation and the U.S. Army is gratefully acknowledged. We are also grateful to Dr. V. Ramamurthy for helpful discussions.

References and Notes

(1) Barashkov, N. N.; Gunder, O. A. *Fluorescent Polymers*; Ellis Horwood: New York, 1994; p 152.
(2) Weber, W. H.; Lambe, J. *Appl. Opt.* **1976**, *5*, 2229.
(3) O'Connell, R. M.; Saito, T. T. *Opt. Eng.* **1983**, *4*, 393.
(4) Nabiokin, Y. V.; Ogurtsova, L. A.; Podgorny, V. P. *Opt. Spectrosc.* **1970**, *28*, 528.
(5) Arnold, M. A. *Anal. Chem.* **1992**, *64*, 1015A.
(6) Gurr, E. *Synthetic Dyes*; Academic Press: New York, **1971**.
(7) Dordick, J.; Marletta, M. A.; Klibanov, A. M. *Biotechnol. Bioeng.* **1987**, *30*, 31.
(8) Akkara, J. A.; Senecal, K. J.; Kaplan, D. L. *J. Polym. Sci., Part A: Polym. Chem.* **1991**, *29*, 1561.
(9) Akkara, J. A.; Samuelson, L. A.; Kaplan, D. L.; Bruno, F. F.; Marx, K. A.; Tripathy, S. K. U.S. Patent 5,143,828, 1992.
(10) Rao, M. A.; John, V. T.; Gonzalez, R. D.; Akkara, J. A.; Kaplan, D. L. *Biotechnol. Bioeng.* **1993**, *140*, 912.
(11) Meister, J. J.; Chen, M.-J.; Chang, F.-F. *Chemtech* **1992**, 431.
(12) Freudenberg, K. *Science* **1965**, *148*, 595.
(13) Kopf, P. W. *Phenolic resins.* In *Encyclopedia of Polymer Science and Engineering*, John Wiley and Sons: New York, 1985; p 11.
(14) Akkara, J. A.; Ayyagari, M.; Bruno, F.; Samuelson, L.; John, V. T.; Karayigitoglu, C.; Tripathy, S.; Marx, K. A.; Rao, D. V. G. L. N.; Kaplan, D. L. *Biomimetics* **1994**, *2*, 331.
(15) Grimme, J.; Schmidt, M. K.; Uckert, F.; Mullen, K.; Scherf, U. *Adv. Mater.* **1995**, *7*, 292.
(16) Burroughes, J. H.; Bardley, D. D. C.; Brow, A. R. *Nature* **1990**, *347*, 539.

(17) Halliwell, B.; Gutteridge, J. M. C. *Free Radicals in Biology and Medicine*; Clarendon Press: Oxford, **1989**.
(18) Pollos, T. L.; Kraut, J. *J. Biol. Chem*. **1982**, *255*, 8199.
(19) Karayigitogulu, C. F.; Kommareddi, N.; Gonzalez, R. D.; John, V. T.; McPherson, G. L.; Akkara, J. A.; Kaplan, D. L. *Mater. Sci. Eng*. **1995**, *C2*, 165.
(20) Ayyagari, M. S.; Marx, K. A.; Tripathy, S. K.; Akkara, J. A.; Kaplan, D. L. *Macromolecules* **1995**, *28*, 5192.
(21) Silverstein, R. M.; Bassler, G. C.; Morrill, T. C. *Spectrometric Identification of Organic Compounds*; John Wiley and Sons: New York, 1981.
(22) Westerfield, W. W.; Lowe, C. *J. Biol. Chem*. **1942**, *145*, 463.
(23) Kuboyama, A.; Kobayashi, F.; Morokuma, S. *Bull. Chem. Soc. Jpn*. **1975**, *48*, 2145.
(24) Jinnouchi, Y.; Kohno, M.; Kuboyama, A. *Bull. Chem. Soc. Jpn*. **1984**, *57*, 1147.
(25) Kuboyama, A.; Arano, H. *Bull Chem. Soc. Jpn*. **1976**, *49*, 1401.
(26) Lindsey, A. S. In *The Chemistry of Quinonoid Compounds*; Patai, S., Ed.; John Wiley and Sons: New York, 1988; Vol. 2, p 841.
(27) Berlman, I. B. *Handbook of Fluorescence Spectra of Aromatic Molecules*; Academic Press: New York, 1971.
(28) Socrates, G. *Infrared Characteristic Group Frequencies*; John Wiley and Sons: New York, 1994.
(29) Ryu, K.; McEldoon, J. P.; Pokora, A. R.; Cyrus, W.; Dordick, J. S. *Biotechnol. Bioeng*. **1993**, *42*, 807.
(30) Pham, P. C.; Lacaze, P. C.; Genoud, F.; Dao, L. H.; Nguyen, M. *J. Electrochem. Soc*. **1993**, *140*, 912.
(31) Gattrell, M.; Kirk, D. W. *J. Electrochem. Soc*. **1992**, *139*, 2736.
(32) Chen, C. L.; Conners, W. J. *J. Org. Chem*. **1974**, *39*, 3877.
(33) Wilkholm, R. J. *J. Org. Chem*. **1985**, *50*, 382.
(34) Sleath, P. R.; Noar, J. B.; Eberlein, G. A.; Bruice, T. C. *J. Am. Chem. Soc*. **1985**, *107*, 3328.
(35) Curtis, M. D.; McClain, M. D. *Chem. Mater*. **1996**, *8*, 945.
(36) Chen, C. L.; Conners, W. J.; Shinker, W. M. *J. Org. Chem*. **1969**, *34*, 2966.

MA960468F